Published in final edited form as:
Phys Med Biol. 2013 June 7; 58(11): 3897–3909. doi:10.1088/0031-9155/58/11/3897.

Usefulness of Ventricular Endocardial Electric Reconstruction from Body Surface Potential Maps to Noninvasively Localize Ventricular Ectopic Activity in Patients

Dakun Lai, PhD[a], **Jian Sun, MD**[b], **Yigang Li, MD**[b], and **Bin He, PhD**[a,c,*]

[a]Department of Biomedical Engineering, University of Minnesota, Minneapolis, USA

[b]Department of Cardiology, Xinhua Hospital Affiliated to Shanghai Jiaotong University School of Medicine, Shanghai, China

[c]Institute for Engineering in Medicine, University of Minnesota, Minneapolis, USA

Abstract

As radio frequency (RF) catheter ablation becomes increasingly prevalent in the management of ventricular arrhythmia in patients, an accurate and rapid determination of the arrhythmogenic site is of important clinical interest. The aim of this study was to test the hypothesis that the inversely reconstructed ventricular endocardial current density distribution from body surface potential maps (BSPMs) can localize the regions critical for maintenance of a ventricular ectopic activity. Patients with isolated and monomorphic premature ventricular contractions (PVCs) were investigated by noninvasive BSPMs and subsequent invasive catheter mapping and ablation. Equivalent current density (CD) reconstruction (CDR) during symptomatic PVCs was obtained on the endocardial ventricular surface in 6 patients (4 men, 2 women, years 23–77), and the origin of the spontaneous ectopic activity was localized at the location of the maximum CD value. Compared with the last (successful) ablation site (LAS), the mean and standard deviation of localization error of the CDR approach were 13.8 mm and 1.3 mm, respectively. In comparison, the distance between the LASs and the estimated locations of an equivalent single moving dipole (SMD) in the heart was 25.5 ± 5.5 mm. The obtained CD distribution of activated sources extending from the catheter ablation site also showed a high consistency with the invasively recorded electroanatomical maps. The noninvasively reconstructed endocardial CD distribution is suitable to predict a region of interest containing or close to arrhythmia source, which may have the potential to guide RF catheter ablation.

Keywords

electrocardiographic inverse problem; current density reconstruction; radio frequency catheter ablation; premature ventricular contraction; body surface potential mapping

1. Introduction

As radio frequency (RF) catheter ablation becomes increasingly prevalent in the management of ventricular tachyarrhythmia in patients, an accurate and rapid determination of the arrhythmogenic site is of important clinical interest, especially for the focal ventricular tachycardia (VT) and symptomatic premature ventricular contraction (PVC),

[*]**Correspondence:** Bin He, PhD, Department of Biomedical Engineering, University of Minnesota, 7-105 NHH, 312 Church Street, Minneapolis, MN 55455, USA, binhe@umn.edu.

which are usually treated with an invasive endocardial surface mapping for detecting those ectopic activities [1,2]. Many efforts have been made in order to estimate noninvasively site of arrhythmia initiation using various electrocardiographic (ECG) inverse solutions, including single moving dipole (SMD) solution [3–7], heart surface activation imaging [8–11], epicardial inverse potential solution [12–14], intramural activation imaging [15–19], and endocardial current density (CD) reconstruction (CDR) [20–25,35]. Following up on our previous animal studies on the recently proposed endocardial CDR approach [25], this study assessed the feasibility of using endocardial CDR approach to localize the initiation site of ventricular ectopic activities in patients with symptomatic PVCs, using noninvasively recorded body-surface potential maps (BSPMs) together with individual heart-torso computed tomography (CT) images. By noninvasively localizing the site of origin of arrhythmia or at least estimating a region of interest containing or close to the arrhythmogenic site before catheterization procedure, the investigated endocardial CDR technique would provide a useful and applicable pre-surgery guideline for operator, and potentially reduce the time needed for detailed catheter mapping.

The aim of the present study was to further assess the performance of endocardial CDR approach in estimating the region critical for maintenance of a clinical ventricular ectopy in patients in order to provide a quantitative measurement of its source localization accuracy. In comparison to previous case reports in patients [20–24] and experimental validations in swine [25], the present study provides the first attempt to quantitatively evaluate the endocardial CDR approach regarding noninvasive localization of ventricular ectopic activity in patients, by comparing with invasive three dimensional (3D) electroanatomical mapping and subsequent successful catheter ablation.

2. Methods

2.1. Subjects

Six consecutive patients (four male, two female patients; age, 58 ± 20 years; range, 23–77 years) were studied. All patients underwent electrophysiological examinations and subsequent RF catheter ablations for symptomatic PVCs. All patients underlying sinus rhythm with PVCs had structurally normal hearts except for one patient who had a previous myocardial infarction and drug-refractory ventricular arrhythmias. Patient characteristics are given in Table 1. All experimental protocols were approved by the Institutional Review Board (IRB) of the XinHua Hospital (affiliated to Shanghai Jiaotong University School of Medicine, Shanghai, China), where data collection was performed, and written informed consent was obtained from all patients.

2.2. ECG mapping

For the body-surface mapping (Figure 1(a), (c), and (e)), BSPMs were recorded in patients with PVCs one day before the ablation. Around 10 minutes of data were collected for each patient. Specifically, 208 conductive-carbon surface electrodes arranged in strips (ActiveTwo system, BioSemi V.O.F, Amsterdam, the Netherlands) were positioned with 144 electrodes on the chest and 64 electrodes on the back. The body-surface electrodes were referenced to the Wilson central terminal. Moreover, an electromagnetic localizer (Fastrak, Polhemus Inc., Colchester, VT, USA) was used to digitize the body-surface electrode positions on the chest while the patient lay in the supine position during the BSPM recording, and on the back as the patient sat upright after the BSPM recording. Three additional fiducial points were located at the precordial, under the left and right armpits, separately, in order to register the digitized body-surface electrodes with CT images.

2.3. Geometric modeling

After BSPM recordings, patients underwent both a thoracic CT scan and a contrast-enhanced cardiac CT angiography scan (ECG gated to 70% of the R-R interval) so as to construct the patient-specific torso and ventricular endocardial geometry (Figure 1(1b) and (1d)). The torso CT data were obtained in four of six patients (not available for patients 3 and 6) with a slice thickness of 7.5 mm and a pixel size of 0.78 × 0.78 mm, and the ventricular geometries were imaged in all patients with a slice thickness of 0.75 mm and a pixel size of 0.39 × 0.39 mm. With the segmented boundaries of the torso, lungs, heart, and the endocardial surfaces of the left ventricle (LV) and right ventricle (RV), an individual numerical volume conductor torso model and the corresponding ventricular endocardial surface model were constructed for each patient (note that a generic torso model was used to co-register with the individual ventricular model in patients 3 and 6). Piecewise isotropic conductivities of 0.2, 0.04, and 0.6 S m^{-1} for the torso, lungs, and heart were used, respectively [26]. Each torso model contained over 4000 triangular boundary elements, and the number of divided small patches on endocardial surface of the LV or RV, which was used for the subsequent current dipole source estimation using the CDR method [20,25], was around 2000–3000. An example of a triangulated heart-torso model obtained from CT data is given in Figure 1(d). Modeling parameters are given in Table 1.

2.4. CDR solutions

The ventricular endocardial CDR method for estimating the cardiac ectopic focus used in this study has been previously described [20,23,35] and rigorously validated in a pacing study in a swine model [25]. By combining body-surface potentials and heart-torso geometric information, the CDR inverse problem was solved with the CURRY software package (Compumedics, Charlotte, NC, USA). Resultantly, the equivalent cardiac source distribution was reconstructed noninvasively on the endocardial surface for the early stage of the ectopic activity (Figure 1(f)). For the relatively small time window of around 20 ms after initiation of an ectopic activity, only the myocardial tissues near the arrhythmogenic site are depolarized, which generate a resultant bioelectric current distribution. Meanwhile, the rest of the heart is still in a resting state, with virtually no electrical activity. The cardiac electric sources from this small area of depolarized myocardia are assumed to be restricted near the ectopy on the endocardial surface. Therefore, the current density distribution on the endocardial surface only of the LV or RV at the early stage of an ectopic activity could approximate the electrical activity of the whole heart [20,25]. Under such assumption, a source model constraint was applied on the endocardium either of the LV or RV on basis of the pattern of BSPMs, and the corresponding ventricular endocardial surface was uniformly divided into couple thousands of small patches. The equivalent current density source model used for ectopic source localization consists of couple thousands of myocardial current dipole sources correspondingly located on these patches. Each of the computed dipoles (at an assigned fixed-location while with arbitrary strength and direction [20,23]) reflects the cardiac electrical activity of the small patch it represents, thus resulting in a spatially segmented image of the cardiac electrical activity, which relates the calculated current dipole distribution of the heart to the recorded body-surface ECGs for the early stage of an ectopic PVC activity (Figure 1(g)).

In this study, the initiation of an early ventricular premature beat was defined as the 0^{th} ms when the magnitude of the measured surface potentials was equal to that of noise (the signal-to-noise ratio (SNR) was equal to 1); then, the onset instant was determined manually at the time when the beginning of an apparent activation could be observed clearly from the ECGs [25]. The resultant cardiac current source, generated by the activated myocardium close to the arrhythmogenic site during early ventricular premature activity, was computed on the constrained endocardial surface of the LV (or RV) in steps of 1 ms after the initiation

of the 0^{th} ms. Specifically, the computed resultant endocardial electrical sources during the early stage of each PVC beat in terms of the magnitude of CD, represented in a spatial resolution of 1 mm, were depicted as CDR maps by means of a color-coded endocardial surface plot of the LV or RV, as labeled with 'CDR Map' shown in Figure 1(g) at the onset instant of a PVC beat coming from RV. Besides the anatomic illustration where an endocardial 'hot spot' region contains or is close to arrhythmogenic sources during the early depolarization of an ectopic activity, we also evaluated the site of maximum value of CDR map (labeled with 'CDR_{max}' in Figure 1(g)), and the optimal site by means of the single moving dipole (SMD) solution (labeled with 'SMD' in Figure 1(g)), for quantitative estimation of the sites of origin of PVC ectopic activity [23,27]. Note that the SMD used to represent cardiac electrical activity is defined as one dipole source, freely movable within the heart, whose resultant body surface potentials would be the closest to the measured one [3–7].

2.5. Statistical analysis

The accuracy of the CDR inverse solution was evaluated in terms of the localization error (LE) of the initiation sites of PVC ectopic beats. In each patient who had PVCs, ventricular endocardial activations were mapped invasively with a 3D electroanatomical mapping system (CARTO, Biosense-Webster Inc., Diamond Bar, CA, USA). After identifying the earliest ventricular activation, characterized as a 'hot spot' in the CARTO map, the RF ablation procedure was performed. Thereafter, all patients were seen in an outpatient clinic with a three-month follow-up. The last (successful) ablation site (LAS) in each patient with PVC was labeled on the CARTO map (labeled with 'LAS' in Figure 1(h)), and its location obtained from contrast venograms and posteroanterior and lateral chest X-rays, was marked on the cardiac CT images by a cardiac electrophysiologist who was blinded to the body surface mapping and inverse solution data [9,28,29]. As such, the location of the LAS within the LV or RV served as a referencewas directly compared with the estimated locations of the maximum CDR point in the resultant heart-torso model (labeled with 'LAS' in Figure 1(g)). The LE statistical analyses, by measuring the 3D distances between the marked LASs and the correspondingly maximum CDR points (and the optimal SMD), were carried out in the resultant heart-torso model over selected 8–10 ectopic beats for each patient, respectively. The overall average distance and standard deviation (SD) were then computed. Additionally, the 'hot spot' CDR map with a threshold set at 90% of the maximum current density (μAmm^{-2}), about the extents of the active cardiac areas at the onset of the PVC complex, was also evaluated qualitatively by comparing that with earlier active areas, as identified from the CARTO activation map [25,27].

3. Results

In ten-minute BSPM recordings, over 1000 PVC beats were identified in six PVC patients (about 200 PVC beats per patient). Of those three patients were found being frequently isolated and monomorphic PVCs (patients 1, 2, and 5), rare but isolated monomorphic PVCs were recorded in two patients (14 beats in patient 3 and 8 beats in patient 6). Moreover, previous infarction was found at the posterior base of the LV in the other patient (patient 4), who had frequent unifocal couplet PVCs. In each patient, RF ablation was performed successfully at one of the following endocardial areas with up to nineteen ablation sites, such as the RV outflow tract (RVOT, in patients 1, 3, 5, and 6), the left coronary cusp (LCC, in patient 2), and the LV Posterior (LVP) base (in patient 4).

Figure 2 shows an example of the reconstructed heart-torso volume conductor model and the body-surface potential measurements in patient 1. This individual heart-torso model consisted of 6,270 triangular boundary elements including the torso, lungs and heart. The endocardial surface of the RV was segmented uniformly into 2406 patches, each of which

was represented by a corresponding pre-fixed dipole source. The displayed ECGs in a butterfly format were recorded during a PVC from 202 surface electrodes (data from six bad channels were excluded). The locations of the body surface electrodes are shown on the volume conductor model (140 electrodes on the front and 62 electrodes on the back, note that 6 bad channels were not included in this model). In Figure 2, the initiation and subsequent onset instant of an early ventricular premature beat are indicated at the 0^{th} ms by a solid black line and the 21^{st} ms by a dash red line in one of the recorded body-surface potential signal waveforms, separately (No. F81 channel, the corresponding electrode of this channel is marked on the volume model). For the surface isopotential maps in figure 2, the isopotential contour lines with an increment of 0.05 mV are depicted with the 202 surface electrodes, which are coupled with the reconstructed heart-torso model. The zero potential contour is indicated by a black curve, and the red lines and the blue lines depict the positive and negative isopotential contour area, respectively. The innermost red or blue contours indicate the positions of the maximum or minimum potentials, specifically. The range for each BSPM is shown as the “P_Range” between the minimum and maximum value of the surface potential. As is shown in the isopotential map, the BSPM indicates a dipolar pattern of the projected cardiac activation on the left-anterior upper surface of the torso at the onset instant. This result was qualitatively in consistency with the corresponding location of the subsequent LAS recorded on the endocardial surface of the RV in CARTO map (Figure 3(a)).

If the morphology of the recorded BSPM data is constantly monomorphic, the early depolarization of ventricular ectopic activity generated by sustained spontaneous arrhythmias should be predictable. Thus, the location of origin of the ventricular ectopy can be preliminarily constrained either in the LV or RV based on the pattern of BPSMs, and further theoretically estimated at a detailed spot or region of the corresponding endocardium using the noninvasive CDR method in one single beat. At various ventricular sites in six patients, noninvasively obtained regions of interest containing or close to arrhythmia sources were estimated and provided as color-coded CDR maps on the endocardium of the RV or LV. Idiopathic and post-infarction PVCs were both investigated. For the endocardial CDR map, the qualitatively distributed information about the extents of the activated areas is identified and shown as a color-coded surface plot of the RV, where current densities are displayed for every patch of endocardial surface of the RV with a threshold set at 90% of the maximum current density moment. Using the procedure described in the evaluation protocol, the performance of CDR localization was thus assessed quantitatively by comparing the predicted locations of origin of PVC beats with the correspondingly recorded LASs in each patient with ten selected beats (except patient 6 with only eight PVCs observed).

Figure 3 shows examples of comparison between the noninvasively estimated results by the CDR/SMD methods and the invasively measured maps by the CARTO mapping system. In figure 3(a), the idiopathic PVCs in patient 1 have been successfully terminated by a RF catheter ablation procedure around the area of the RVOT. By applying the CDR inverse analysis on the BSPMs collected before ablation, the CDR map was estimated for the early PVC activity (during the time window of 0–21 ms corresponding to the PVC beat shown in figure 2). For the onset instant of the 21^{st} ms after the initiation of 0^{th} ms, a small area of CDR map (yellow area), the maximum CDR point (red dipole), and the optimal SMD (blue dipole) all were estimated around the area of the RVOT, where a successful ablation was performed (green ball). Qualitatively, the ‘hot spot’region of CDR map (yellow in the left panel of the Figure 3(a)), predicated at the RVOT, agreed approximately with the view of the corresponding endocardial ‘hot spot’ activation map (about 0–25 ms, red in the lower-right panel of the Figure 3(a)) exported from the invasive CARTO system. The predicated ‘hot spot’ area almost centrally contained the actual arrhythmia source identified with the

LAS as marked on cardiac CT images blindly by a cardiac electrophysiologist (in the upper-right panel of the Figure 3(a)). Furthermore, the location of the maximum value point observed from the 'hot spot' CDR map and the position of the optimal SMD both coincided with the position of the LAS. Moreover, in a large number of collected beats, this finding was repeatedly demonstrated and no significant differences concerning this consistency were found in patients 2, 4, and 5, although a slight beat-to-beat uncertainty of LEs was observed, as given in Table 2. It is also noteworthy that there is a small difference in the shape, area, and location of the 'hot spot' between the estimated CDR map and the measured 'hot spot' area of the CARTO activation map. Particularly, a lower magnitude of the estimated maximum endocardial current density (1.00 μAmm^{-2}) and a relative larger area of the 'hot spot' CDR map were observed around the LVP in the post-infarction area in patient 4, compared with other patients who had idiopathic PVC in a higher magnitude of over 2.00 μAmm^{-2} (Figure 3(b)). The actual measured infarction area and the LAS were shown in the corresponding CARTO endocardial voltage map (a threshed of 0.5 mV, red in the right panel of Figure 3(b)). In the absence of individual thoracic CT images, the recorded PVC data in patients 3 and 6 were analyzed with a co-registered generic torso model and the individual ventricular endocardial model. Figure 3(c) shows an example of the estimated locations of a PVC arrhythmia initiation with a generic torso model by the CDR/SMD methods, which was further evaluated by comparing with the location of the LAS shown on the CARTO map. In figure 3(c), a catheter ablation procedure was performed successfully around the area of the RVOT near the septum in patient 3. The 'hot spot' CDR area and the corresponding maximum CDR point of the map at the PVC onset instant were both estimated approximately at the RVOT near the free wall, while away from the actual area of the septum, as shown in the CARTO map in right panel of Figure 3(c). Although the estimated CDR results showed insignificant correlations with the recorded CARTO map and the location of the LAS, the estimated CDR maps during PVCs were adjacent to the arrhythmia sources as defined by the LAS.

Table 2 gives statistical analyses on the inversely computed origins of pre-excitation by comparing the invasively recorded locations of LASs, in terms of the LEs of a total of 58 PVC beats in six patients with and without an individual torso model. For those 4 patients who have a patient-specific heart-torso model, a total of 40 PVC beats including 30 of the idiopathic PVC (patients 1, 2, and 5) and 10 of the post-infarction PVC (patient 4) were analyzed, and the corresponding average CDR LEs and SMD LEs both were statistically calculated as shown in Table 2. Regardless of possible identification error of the LAS from the biplane X-ray, the CDR-localized catheter positions were reliably consistent with the successful ablation site to an accuracy of 10.9 ± 1.4 mm, which is significantly smaller than the accuracy of 22.6 ± 4.8 mm for the SMD method. Additionally, in both of patients (patients 3 and 6) without their thoracic CT images, relatively larger LEs of ±20 mm were observed due to the generic torso model used in these 2 patients as compared with that of ±11 mm of other patients using a patient-specific heart-torso model. As summarized in Table 2, the LEs in 18 selected PVC beats (10 beats from patient 3 and 8 beats from patient 6) are 19.4 ± 1.1 mm and 31.3 ± 7.0 mm for the CDR and SMD methods, respectively.

4. Discussion

Localization of site of arrhythmia initiation has direct clinical benefits for better understanding the underlying mechanisms of cardiac pathophysiology, and potentially guiding therapeutic treatments of cardiac arrhythmia in a cardiac electrophysiology lab. The present results suggest that the endocardial CDR approach is feasible to inversely reconstruct cardiac electrical events of focal ventricular tachyarrhythmia in patients from the measured BSPMs, and thus directly and noninvasively to estimate the location of origin of the ventricular ectopic activity in terms of the reconstructed CD distribution on the

endocardial surface. Using the reconstructed endocardial CDR maps, the earlier ventricular depolarization initiated by a unifocal PVC was able to be identified and located around the actual ectopic foci on the endocardial surface of the corresponding ventricle. By using a quantitative measurement in terms of the maximum CD point of estimated CDR maps, the patients' data presented in this study further indicate the localization accuracy of the endocardial CDR at ±15mm, which is comparable to our previously published experimental data that have been rigorously validated in an *in vivo* swine model [25]. Moreover, the agreement of clinical findings from invasive catheter mapping and ablation with the estimated location of the successful ablation site corroborates well the noninvasive CDR findings.

A statistical and clinical validation of the noninvasive endocardial CDR approach in cardiac source localization has not been reported so far, and initial results are available only for case reports in the human [20–24]. In 2001, Leder *et al* calculated the pathway of atrio-ventricular pre-excitation with MCGs in a patient suffering from WPW syndrome [21]. Their one-patient case report showed that the CDR solution in terms of the location of the highest current density has a good source localization ability at the early stage of the delta wave (15–35 ms) by comparing with the site of catheter ablation. Similar investigations of the endocardial surface CDR localization have been performed on the individual LV surface in patients suffering from previous myocardial infarction (MI) [22,24,35], coronary artery disease (CAD) [20], and sustained VT [23].

The present study was carried out to evaluate the performance of the endocardial CDR approach in detecting the location of ventricular arrhythmia initiation in six patients who underwent subsequent RF catheter ablations for symptomatic PVC. 3D invasively endocardial electroanatomical mapping and successful catheter ablation were performed in each of six patients with either idiopathic or post-infarction PVC. The catheter position of the successful LAS was verified by X-ray imaging and the stability was assured by repeated short fluoroscopy, which served as a reference for the correct CDR localization. Major findings of this study include the following. First, a total of 58 PVC beats were analyzed in all of six patients, and the average LEs of the estimated source of ectopic activities at the onset instant (around the 20^{th} ms after the initiation of the 0^{th} ms for all of beats) were 13.8 ± 1.3 mm for the CDR approach (1 mm, the spatial resolution of the endocardial source distribution) and 25.5 ± 5.5 mm for the SMD method (within a 3D solution space of the whole heart), respectively. Although there exist some identification error of the LAS from X-ray images [28,29], the CDR-localized sites of initiation of PVCs were consistent with the successful ablation site at an average accuracy of ±12 mm in total of 40 beats of four patients who have patient-specific heart-torso models. Note the larger LEs of ±20 mm in two patients (patients 3 and 6) due to numerical modeling error employing a generic torso model without individual thoracic CT images. The obtained results indicate an improved ability of the CDR technique to localize the early endocardial ectopic activity, compared to the well studied SMD localization method. Second, In addition to the quantitative arrhythmia source localization, the 'hot spot' area estimated by the CDR method contained, or was at least close to the actual arrhythmia sources. As such, the CDR technique with a 3D reconstructed CDR map on the specific endocardium could give cardiologists more precise information where the focus of an ectopic activity lies. Third, similar performance of the endocardial CDR localization was observed among multiple beats in the same patient (beat-to-beat uncertainty of ±2 mm) at both endocardial surfaces of the LV (LCC, LVP) and RV (RVOT), and in different conditions including isolated idiopathic PVCs and unifocal couplet PVCs after infarction. On the other hand, although these six recruited patients suffered from different types of ventricular pre-excitation as described above, there was no evidence found that those specific conditions played a role for the CDR approach in cardiac source localization in this pilot clinical study.

Furthermore, advantages of this study include the following, by comparing with the previous reports and related ECG inverse solutions. First, employing the invasive endocardial mapping and ablation data to quantitatively evaluate the endocardial CDR approach in patients represents a unique feature of the present study. Since the endocardial surface current density source model considers equivalent sources only on the endocardial surface of the LV or RV, the clinically recorded endocardial surface CARTO maps provide a desired means of assessing this CDR method. Second, compared with the other established source localization methods with an inverse model either in the whole volume of the heart or on the epicardial/endocardial surface of the ventricles [8–19], the endocardial CDR approach validated in this study also shows a relatively higher computational efficacy with a source model constraint applied only on the endocardium of the LV or RV. Third, in contrast with described inverse solutions directly with detailed cardiac geometries and performed in one single beat, the conventional indirect mapping and localization techniques that compare the BSPMs or 12-leads standard ECGs with databases, demands considerable experience on pattern recognition, and are time-consuming, especially when treating poorly tolerated or non-inducible VT [30–34]. The present study suggests that the ECG inverse endocardial surface CDR approach would provide a rapid and noninvasive determination of the region critical for maintenance of a clinical ventricular ectopy in patients from a single-beat BSPMs, and potentially provides a useful complementary, noninvasive localization approach for catheter based mapping and ablation of cardiac arrhythmias.

Study Limitations

In this study, the endocardial surface CDR approach may be limited in that it does not account for the 3D nature of cardiac electrical activity and the anisotropic nature of myocardium. Therefore, estimation errors may be introduced as well, due to such simplification of the anisotropic myocardium in the numerical torso model and neglect of the contribution of the 3D myocardial activation involving different myocardial layers even in the early activation stage [18,36]. Moreover, the clinical validation of CDR is limited by the finite accuracy of the reference itself. Even if our results showed no significant difference concerning the LEs between our previous pacing studies in a rigorous near-clinical setting and present PVC studies with marked LASs on the basis of biplane X-ray images, there exist errors in the determination of successful ablation sites from co-registration of CT data with the CARTO data [37]. Recent developments in CARTOMERGE technique (Biosense-Webster Inc., Diamond Bar, CA, USA) suggest the possibility that the actual LASs and estimated initiation sites can be possibly shown on the same CARTO-CT merge image and thus decreasing the co-registration error in future investigations. Meanwhile, the patient population ($n = 6$) included in this study is small for statistical evaluation, and endocardial CDR localization was carried out in only one patient with post-infarction PVC. Additionally, this study applied a preliminary source constraint on the endocardial surface either of the LV or RV to reconstruct the endocardial source distribution of ventricular ectopic activities. Thus, one should be cautious when using CDR maps with multiple ‘hos spots’ or patchy CD distributions to localize the initial site of such cardiac ectopic activity, especially for the polymorphic ventricular ectopic activity or multiple foci existing in both of the LV and RV. However, this study is the first attempt to systematically apply endocardial CDR in a cohort of patients undergoing treatment for a symptomatic ventricular arrhythmia. Further investigations in a larger patient population, especially with various ventricular arrhythmias, such as VT, post-infarction PVC, frequent PVC, and rare PVC, etc., may establish its clinical validity and applicability.

5. Conclusions

In conclusion, the present study indicates the utility of the ventricular endocardial electric reconstruction for localization of the site of origin of ventricular ectopic activity in patients underlying sinus rhythm with idiopathic PVCs. The present pilot clinical results suggest that the endocardial CDR approach may offer the possibility of providing an easy and inexpensive clinical pre-diagnosis of focal arrhythmias with sub-endocardial origins, guiding initial placement of endocardial mapping, and aiding catheter ablation of ventricular arrhythmias.

Acknowledgments

The authors are grateful to Zhaoye Zhou, Dr. Quanshan Wang, and Dr. Qiufeng Lu for assistance in data collection. This work was supported in part by NIH RO1HL080093 and NSF CBET-0756331, and a grant from the Institute of Engineering in Medicine from the University of Minnesota.

References

1. Morady F. Radio-frequency ablation as treatment for cardiac arrhythmias. N Engl J Med. 1999; 340:534–544. [PubMed: 10021475]
2. Friedman PA. Novel mapping techniques for cardiac electrophysiology. Heart. 2002; 87:575–582. [PubMed: 12010949]
3. Gulrajani RM, Huy-Pham H, Nadeau RA, et al. Application of the single moving dipole inverse solution to the study of the Wolff-Parkinson-White syndrome in man. J Electrocardiol. 1984; 17:271–288. [PubMed: 6481281]
4. Ideker RE, Bandura JP, Larsen RA, Cox JW, Keller JW, Brody DA. Localization of heart vectors produced by epicardial burns and ectopic stimuli: Validation of a dipole ranging method. Circ Res. 1975; 36:105–112. [PubMed: 1116214]
5. Armoundas AA, Feldman AB, Mukkamala R, et al. Statistical accuracy of a moving equivalent dipole method to identify sites of origin of cardiac electrical activation. IEEE Trans Biomed Eng. 2003; 50:1360–1370. [PubMed: 14656065]
6. Savard P, Roberge FA, Perry JP, Nadeau RA. Representation of cardiac electrical activity by a moving dipole for normal and ectopic beats in the intact dog. Cir Res. 1980; 46:415–425.
7. Lai D, Liu C, Eggen ME, Iaizzo PA, He B. Equivalent moving dipole localization of cardiac activity in a swine model during pacing. IEEE Trans Info Tech Biomed. 2010; 14:1318–1326.
8. Tilg B, Fischer G, Modre R, et al. Model-based imaging of cardiac electrical excitation in humans. IEEE Trans Med Imaging. 2002; 21:1031–1039. [PubMed: 12564871]
9. Berger T, Fischer G, Pfeifer B, et al. Single-beat noninvasive imaging of cardiac electrophysiology of ventricular pre-excitation. J Am Coll Cardiol. 2006; 48:2045–2052. [PubMed: 17112994]
10. Huiskamp G, Greensite F. A new method for myocardial activation imaging. IEEE Trans Biomed Eng. 1997; 44:433–446. [PubMed: 9151476]
11. Dam PM, Oostendorp TF, Linnenbank AC, Oosterom AV. Non-invasive imaging of cardiac activation and recovery. Ann Biomed Eng. 2009; 37:1739–1756. [PubMed: 19562487]
12. He B, Wu D. A bioelectric inverse imaging technique based on surface Laplacians. IEEE Trans Biomed Eng. 1997; 44:529–538. [PubMed: 9210812]
13. Burnes JE, Taccardi B, Rudy Y. A noninvasive imaging modality for cardiac arrhythmias. Circulation. 2000; 102:2152–2158. [PubMed: 11044435]
14. Ghost S, Rhee EK, Avari JN, Woodard PK, Rudy Y. Cardiac memory in patients with Wolff-Parkinson-White syndrome: noninvasive imaging of activation and repolarization before and after catheter ablation. Circulation. 2008; 118:907–915. [PubMed: 18697818]
15. He B, Li G, Zhang X. Noninvasive three-dimensional activation time imaging of ventricular excitation by means of a heart-excitation-model. Phys Med Biol. 2002; 247:4063–4078. [PubMed: 12476982]

16. Zhang X, Ramachandra I, Liu Z, Muneer B, Pogwizd SM, He B. Noninvasive three-dimensional electrocardiographic imaging of ventricular activation sequence. Am J Physiol- Heart and Circulatory Physiology. 2005; 289:H2724–H2732.
17. Liu C, Skadsberg ND, Iaizzo PA, He B. Estimation of global ventricular activation sequences by noninvasive three-dimensional electrical imaging: validation studies in a swine model during pacing. J Cardiovascular Electrophysiology. 2008; 19:535–540.
18. Han C, Pogwizd S, Killingsworth CR, He B. Noninvasive imaging of three-dimensional cardiac activation sequence during pacing and ventricular tachycardia. Heart Rhythm. 2011; 8:1266–1272. [PubMed: 21397046]
19. He B, Wu D. Imaging and visualization of 3D cardiac electric activity. IEEE Trans Info Technol Biomed. 2001; 5:181–186.
20. Leder U, Pohl HP, Michaelsen S, et al. Noninvasive biomagnetic imaging in coronary artery disease based on individual current density maps of the heart. Int J Cardio. 1998; 64:83–92.
21. Leder U, Haueisen J, Pohl P, et al. Methods for the computational localization of atrio-ventricular pre-excitation syndromes. Int J Cardiovasc Imaging. 2001; 17:153–160. [PubMed: 11558974]
22. Leder U, Haueisen J, Pohl P, et al. Localization of late potential sources in myocardial infarction. Int J Cardiovasc Imaging. 2001; 17:315–325. [PubMed: 11599871]
23. Muller HP, Godde P, Czerski K, et al. Localization of a ventricular tachycardia-focus with multichannel magnetocardiography and three-dimensional current density reconstruction. J Med Eng Tech. 1999; 23:108–115.
24. Nenonen J, Pesola K, Hanninen H, et al. Current-density estimation of exercise-induced ischemia in patients with multivessel coronary artery disease. J Electrocardiol. 2001; 34:37–42. [PubMed: 11781934]
25. Lai D, Liu C, Eggen MD, Iaizzo PA, He B. Localization of endocardial ectopic activity by means of noninvasive endocardial surface current density reconstruction. Phys Med Bio. 2011; 56:4161–4176. [PubMed: 21693786]
26. Geddes LA, Baker LE. The specific resistance of biological material: a compendium of data for the biomedical engineer and physiologist. IEEE Trans Biomed Eng. 1967; 5:271–293.
27. Bai X, Towle VL, He EJ, He B. Evaluation of cortical current imaging methods using intracranial electrocardiograms and functional MRI. NeuroImage. 2007; 35:598–608. [PubMed: 17303438]
28. Hauer RNW, Heethaar RM, de Zwart MTW, et al. Endocardial catheter mapping: validation of a cineradiographic method for accurate localization of left ventricular sites. Circulation. 1986; 74:862–868. [PubMed: 3757194]
29. McClelland AJJ, Owens CG, Navarro C, et al. Usefulness of body surface maps to demonstrate ventricular activation patterns during left ventricular pacing and reentrant activation during ventricular tachycardia in men with coronary heart disease and left ventricular dysfunction. Am J Cardio. 2006; 98:591–596.
30. He B, Cohen RJ. Body surface Laplacian mapping of cardiac electrical activity. Am J Cardio. 1992; 70:1617–1620.
31. He B, Wu D. Laplacian electrocardiography. Critical Reviews in Biomedical Engineering. 1999; 27:285–338. [PubMed: 10864282]
32. He B, Wu D. A bioelectric inverse imaging technique based on surface laplacians. IEEE Trans Biomed Eng. 1997; 44:529–538. [PubMed: 9210812]
33. SippensGroenewegen A, Spekhorst H, van Hemel NM, et al. Localization of the site of origin of postinfarction ventricular tachycardia by endocardial pace mapping. Body surface mapping compared with the 12-lead electrocardiogram. Circulation. 1993; 88:2290–2306. [PubMed: 8222124]
34. Peeters HAP, SippensGroenewegen A, Wever EFD, et al. Clinical application of an integrated 3-phase mapping technique for localization of the site of origin of idiopathic ventricular tachycardia. Circulation. 1999; 99:1300–1311. [PubMed: 10077513]
35. Leder U, Haueisen J, Huch M, Nowak H. Non-invasive imaging of arrhythmogenic left-ventricular myocardium after infarction. The Lancet. 1998; 352:1825.

36. Ramanathan C, Rudy Y. Electrocardiographic imaging: II. effect of torso inhomogeneities on the noninvasive reconstruction of epicardial potentials, electrograms and isochrones. J Cardiovascular Electrophysiology. 2001; 12:241–252.

37. Cuculich PS, Wang Y, Lindsay BD, et al. Noninvasive characterization of epicardial activation in humans with diverse atrial fibrillation patterns. Circulation. 2010; 122:1364–1372. [PubMed: 20855661]

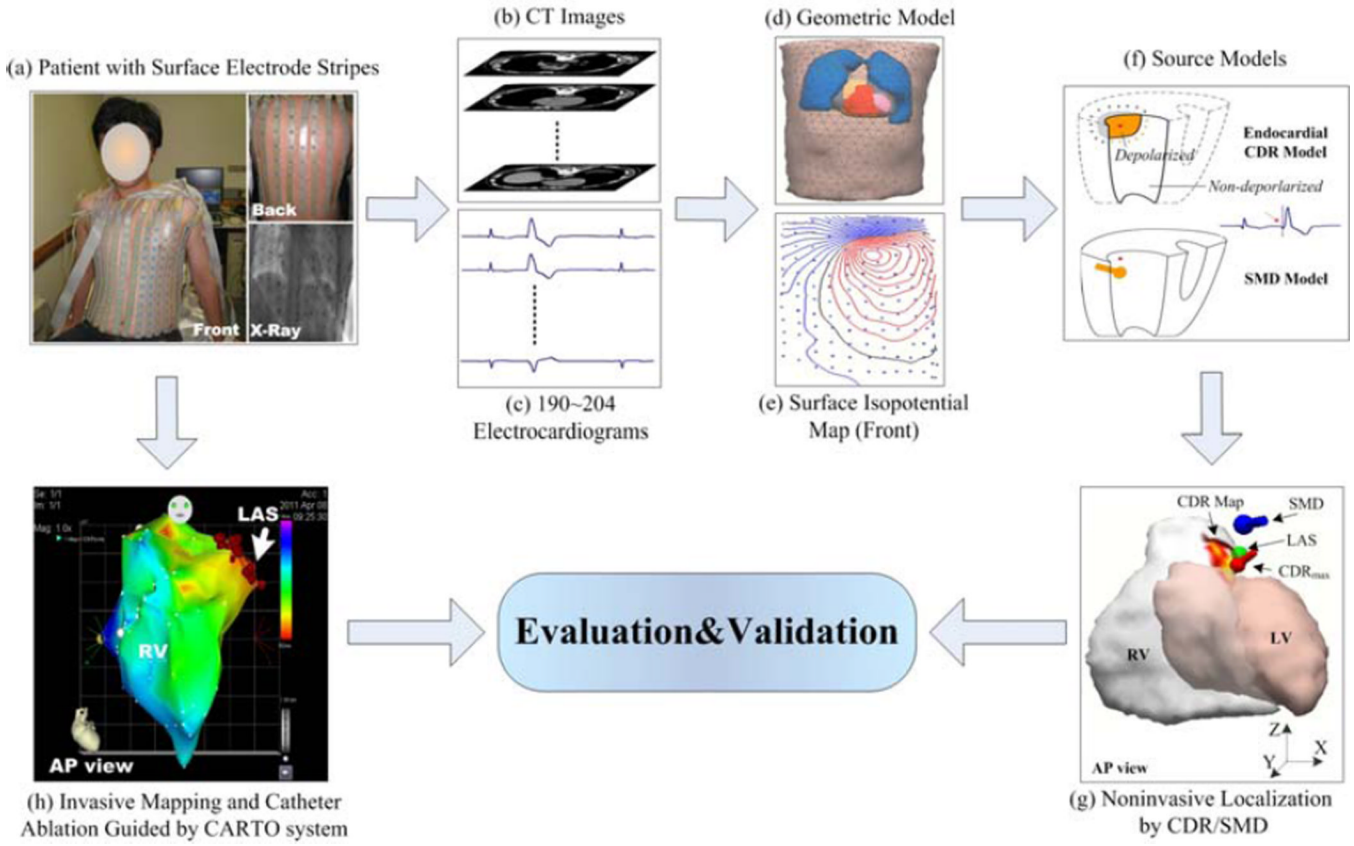

Figure 1.

Schematic diagram of ECG inverse solution and evaluation procedure. LV and RV represents the endocardial surface of the left and right ventricular, respectively, AP view represents anterior-posterior view, CDR model represents the inverse electrocardiographiccurrent density reconstruction method, SMD model represents the signal moving dipole method, CDR_{max} represents the maximum point of the estimated current density map, SMD represents the estimated origin of the ectopic activity by the SMD method, LAS represents the successful last ablation sitelabeled on the CARTO map and its location was marked on the cardiac CT images blindly by a cardiac electrophysiologist on basis of contrast venograms and posteroanterior and lateral chest X-rays, and CDR Map represents the estimated ‘activation distribution’ of the ectopic activity on the ventricular endocardial surface using the CDR method.

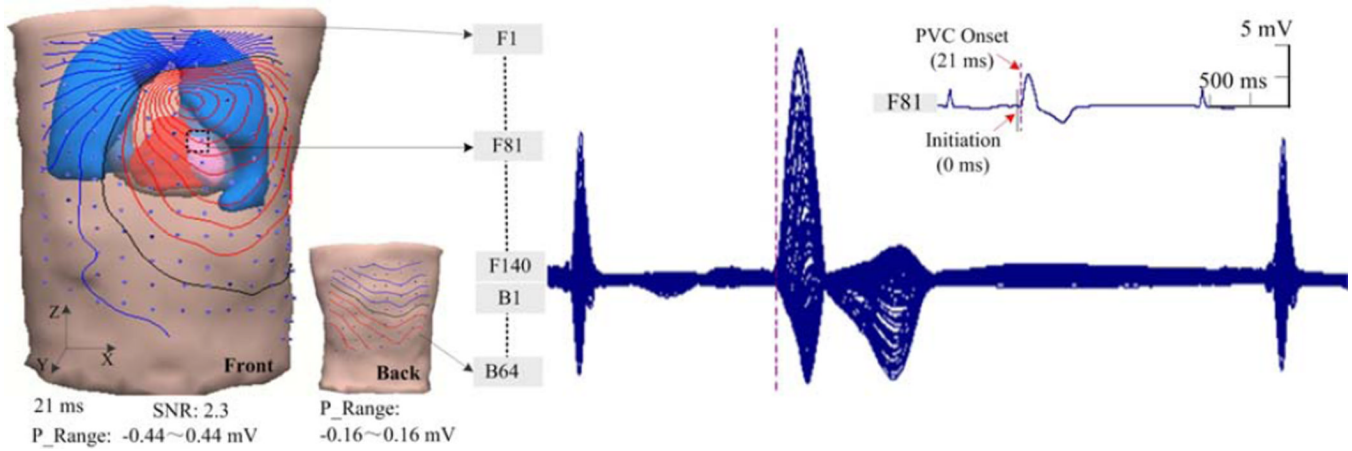

Figure 2.

A heart-torso model with illustration of coupled body-surface electrode positions on the front and back and the recorded surface ECGs in a butterfly format during a premature ventricular complex at the RVOT. The surface isopotential map is depicted with effective surface electrodes by the increment of 0.05 mV.

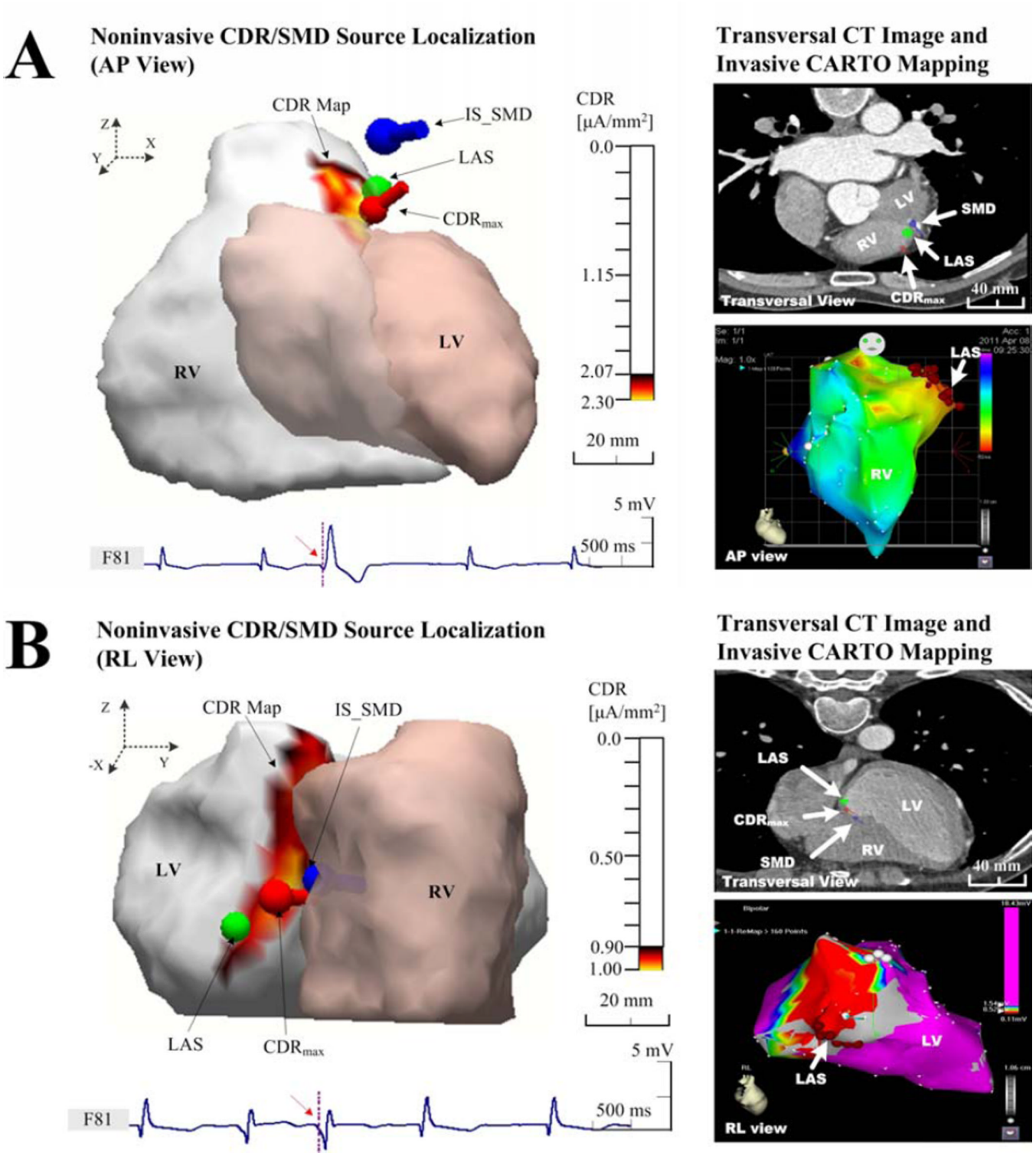

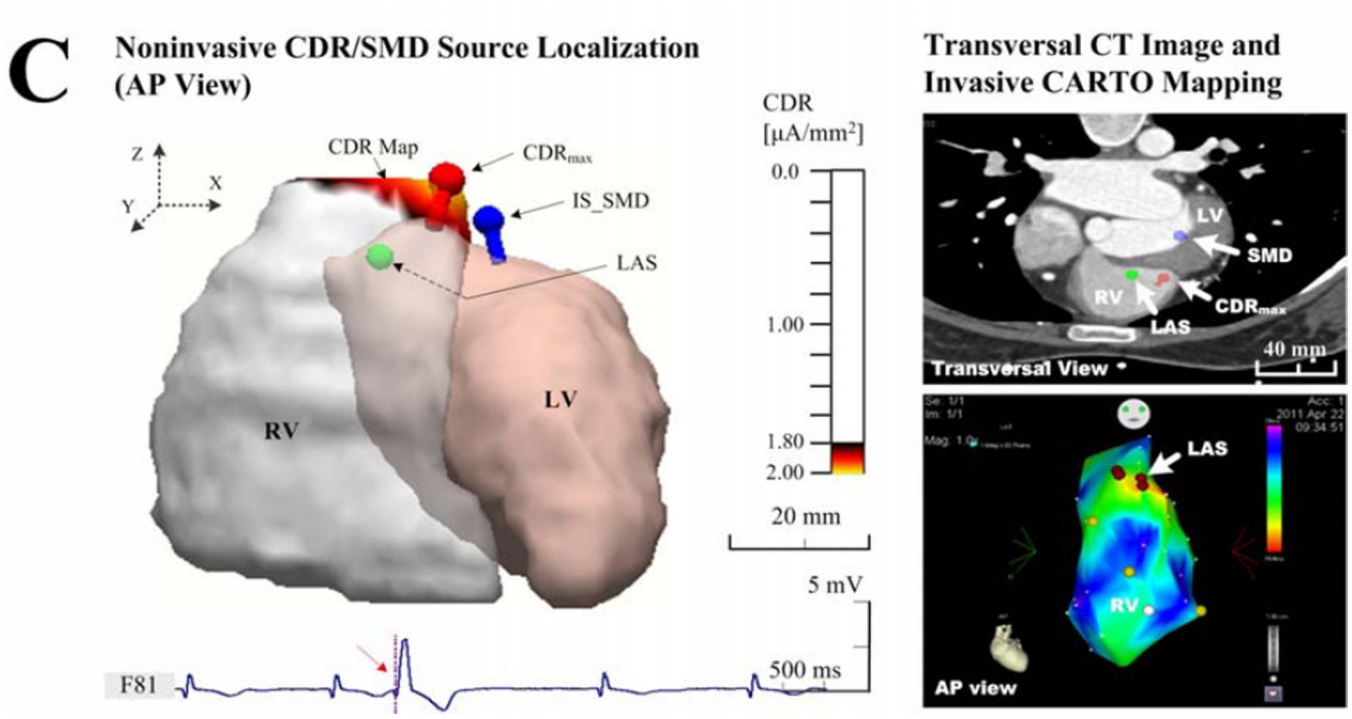

Figure 3.

Examples of the endocardial CDR localization. (a) Results in patient 1 with an individual torso model, who had frequently idiopathic PVCs at the RVOT; (b) Results in patient 4 with an individual torso model, who had frequently unifocal couplet PVCs after infarction at the LVP; and (c) results in patient 3 with rare idiopathic PVCs at the RVOT but solved with a generic torso model. The sub-figures include the 'Noninvasive CDR/SMD Source Localization' and the 'Transversal CT Images and invasive CARTO Mapping'. Each right panel shows the view of the corresponding activation (a and c) or potential (b) map directly recorded by the invasive CARTO system, and the LAS was labeled on the corresponding map and markedon the CT image blindly by a cardiac electrophysiologist on basis of biplane X-ray images. The estimated current densities are displayed on the endocardial surface for every patch of the LV or RV with a threshold set at 90% of the maximum dipole moment ($\mu A/mm^2$).

Table 1

Patient characteristics and modeling parameters[a]

Patient No Gender	Patient Age (yrs)	Patient Conditions	Initial Site ofEctopy	PVCs Count (n / 24 Hrs)	Ablation Sites (n)	Electrodes Used (n)	Torso Model (n)	Source Model (n)
1, Male	45	Idiopathic PVC	RVOT	≥35000	19	202	6270	2406
2, Male	77	Idiopathic PVC	LCC	≥26000	12	194	5190	2004
3, Female	23	Idiopathic PVC	RVOT	≥4000	4	191	4328[b]	2868
4, Male	53	PVC after MI	LVP	≥58000	6	198	5608	2218
5, Male	75	Idiopathic PVC	RVOT	≥37000	9	198	5490	3110
6, Female	46	Idiopathic PVC	RVOT	≥2000	5	195	4238[b]	3178
Mean ± SD	58 ± 20	—	—	—	9 ± 6	198± 5	5345 ± 725	2500± 480

[a]Data are presented as absolute values. PVC, premature ventricular contraction, MI, myocardial infarction; RVOT, right ventricular outflow tract; LCC, left coronary cusp; LVP, left ventricular posterior base;

[b]Generic torso model from a female subject was used asno individual torso CT scans available.

Phys Med Biol. Author manuscript; available in PMC 2014 June 07.

Table 2

LEs of the endocardial CDR method and SMD approach for identifying the site of origin of focal ventricular ectopy in six patients with and without an individual torso model[a]

Patient No Ectopic site	Beat-to-beat CDR Estimation Uncertainty (mm)										Average CDR LEs (mm)	A verage SMD LEs (mm)
	1	2	3	4	5	6	7	8	9	10		
PVC beats with an individual torso model												
1, RVOT	14.2	10.3	12.1	13.2	14.3	15.8	12.4	15.4	11.8	15.0	13.8 ± 1.4	25.5±4.7
2, LCC	13.5	15.4	13.6	15.5	11.2	13.3	11.1	11.0	13.5	13.5	13.2 ± 1.6	22.0±6.8
4, LVP	10.3	5.3	7.7	7.9	5.5	4.5	8.2	5.0	8.2	9.6	7.2 ± 2.0	23.2± 3.9
5, RVOT	9.2	9.9	9.5	10.2	9.2	10.3	9.6	9.2	10.0	9.2	9.5 ± 0.4	19.7±3.7
PVC beats with a generic torso model												
3, RVOT	20.8	21.4	19.8	20.9	21.0	19.4	21.7	21.4	19.0	20.3	20.5 ± 0.9[b]	29.7± 7.4[b]
6, RVOT	17.5	19.6	19.0	19.2	19.0	16.9	16.1	19.3	—	—	18.3 ± 1.3[b]	32.9± 6.5[b]

[a]LE, Localization error; CDR, current density reconstruction; SMD, single move dipole; Average CDR or SMD Localization Error, the mean distances (mm) over eight-ten beats between the location of the maximum current density point or the optimal SMD and the successful ablation site in patients with PVCs

[b]Results were obtained in a patient specific heart model and a generic torso model.